

A NEW LOAD FREQUENCY CONTROL METHOD IN POWER SYSTEM USING VEHICLE-TO-GRID SYSTEM CONSIDERING USERS' CONVENIENCE

Koichiro Shimizu*, Taisuke Masuta, Yutaka Ota, and Akihiko Yokoyama
The University of Tokyo
Tokyo, Japan
shimizu@syl.t.u-tokyo.ac.jp

Abstract – A large penetration of photovoltaic and wind power generation causes the imbalance between supply and demand in power systems because their output is intermittent. To alleviate the mentioned problem, many researches on Load Frequency Control (LFC) using Electric Vehicles (EVs) as controllable loads have been studied. In this paper, we propose a new LFC method using EVs, which is named the State Of Charge (SOC) synchronization control. In the control method, a number of EVs can be considered as one large-capacity battery energy storage system. Moreover, the EVs are plugged-in/out anytime when the users like and store the sufficient energy for the next trip at plug-out. This paper shows the modeling of the EVs and the evaluation of the control method.

Keywords: *Battery Energy Storage System (BESS), Electric Vehicle (EV), renewable energy, smart grid, Vehicle-to-Grid (V2G), Load Frequency Control (LFC)*

1 INTRODUCTION

Recently, photovoltaic generation and wind power generation have become the most popular renewable energy based generation for solving the environmental problems such as greenhouse gas emission throughout the world. However, their power generation cannot be kept constant and sometimes cause the imbalance between supply and demand in power systems. To alleviate the mentioned problem, a large-capacity of Battery Energy Storage System (BESS), which is significantly expensive, is indispensable. Therefore, many researches on the contribution of controllable loads such as heat pump water heaters and Electric Vehicles (EVs) to the Load Frequency Control (LFC) have been studied for the reduction of the BESS installation. In this paper, the EVs are considered as controllable loads.

EVs which have electric motors instead of engines have gained much attention as the next generation vehicles. EVs can be controlled such as BESS in the grid because the batteries of EVs with two-way power converters can be charged and discharged corresponding to a control signal from the Central Load Dispatching Center (CLDC). EVs are now expected to be charged or discharged with the reasonable control scheme to solve the problems caused by a large penetration of renewable energy, e.g. surplus power, frequency fluctuation and voltage rise [1][2]. In this paper, the problem afflicted with the frequency is focused.

Our research is based on Vehicle-to-Grid (V2G) which is a concept of charging and discharging between the batteries of the EVs and the power system in order to contribute to the power system operation and control. Especially in this paper, the EVs are under the centralized control with a two-way communication network between the EVs and the power system. It is assumed that the CLDC sends the control signal to the EVs and receives the information from the EVs via the Local Control centers (LC centers). There are two problems in the V2G because the EVs are not control equipment on the supply side like BESS but users' equipment on the demand side. The first one is the EV users' convenience. The EVs should be plugged-in/out anytime when the users like and should store the sufficient energy at plug-out for the next trip. The second one is the EV users' uncertainty. State Of Charge (SOC) of the batteries is different from EV to EV. When some EVs stop charging/discharging due to their full/empty battery energy or being plugged-out, the performance of the power system control using the EVs becomes worse. The power system needs to reduce the risk of such uncertainty.

In this paper, a lumped EV model is designed considering EV users' convenience and uncertainty. Moreover, a frequency control method based on the lumped model is proposed. In addition, a dispatching method of the control signal (LFC signal) to the EVs, which enables the SOC of all the EVs to be synchronized, is proposed. Effectiveness of the control proposed methods is evaluated by numerical simulations conducted on the power system model. It is assumed in this paper that EVs can both charge and discharge via usual outlets such as household wall outlet and that such outlets are sufficiently installed to car parks at offices, supermarkets, etc. in the future. Charging infrastructure such as quick charger/discharger is not necessary.

2 SOC SYNCHRONIZATION CONTROL

2.1 The states of EV

All the EVs respond to the LFC signal after completing to charge batteries to a sufficient level. As shown in Fig. 1, three main states of EVs are defined in this paper, i.e. driving, charging, and controllable states. Furthermore, there are three transitions from state to state,

i.e. plug-in, plug-out, and control-in. Each state and transition is described in details as follows:

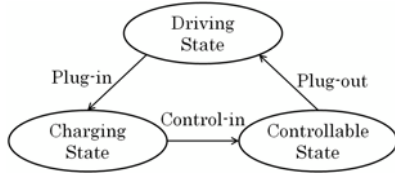


Figure 1: State and transition of the EV.

An EV transits from the controllable state to the driving state (plug-out) for the trip. In the driving state, the EV is on road and disconnected from the power system.

An EV transits from the driving state to the charging state (plug-in) after the trip to charge its battery. Such EV cannot yet respond to the control signal from the power system, i.e. it is uncontrollable.

An EV transits from the charging state to the controllable state (control-in) to respond to the control signal from the power system. The SOC of the EVs fluctuate depending strongly on the signal. In this paper, however, the EVs are controlled within the SOC of the EVs between 80% and 90%. Therefore, the EVs are plugged-out with the sufficient energy for the next trip anytime when the uses like.

An EV has a difficulty in going on a long trip because the driving distance of an EV per one charging is shorter than that of a gasoline vehicle per one fill. On the other hand, an EV can be easily charged everywhere, i.e. at a garage, at a parking lot of an office or a supermarket, although a gasoline vehicle can be filled up only at a gas station. Therefore, it is expected that the EV users intend to charge frequently. In general, there are only a few cars driving on road in contrast to the number of cars not driving especially in Japan [3]. That is to say, almost all the cars are usually parked and this situation is expected to be the same in the future with a large penetration of the EVs. As a result, almost all the EVs are plugged with nearly full SOC. Although the number of the EVs in the controllable state changes according to the mobility behavior of the EVs, it is expected to be large enough for the LFC. In this paper, only the EVs in the controllable state are controlled.

2.2 SOC synchronization control

An SOC synchronization control method, which enables the SOC of the EVs to be synchronized, is presented in this subsection. The SOC of the battery of an EV is equivalent to the amount of gasoline tank of a conventional vehicle. The control method enables us to treat a number of the EVs as one large-capacity BESS.

It is assumed that the CLDC sends the control signal to the EVs and receives the information from the EVs via the LC center. As shown in Fig. 2, it is assumed that there are 500 local control centers and 50,000 EVs in the study area. Each local control center is assumed to control 100 EVs. The SOC synchronization control system consists of the system between the CLDC and the LC centers (upper layer) and that between the LC centers and the EVs (lower layer). The CLDC receives

the information on the sum of the inverter capacity of the EVs and the synchronous SOC (discussed in section 3.1) from the LC centers. The EVs send the information on their states when the EVs change those to or from the controllable state (control-in, plug-out). In addition, the EVs send the SOC to the LC center every 30 seconds. The CLDC calculates the LFC signal from the frequency fluctuation. In this paper, the CLDC dispatches the LFC signal to the LC centers by the dispatching method in the upper layer. The LC centers dispatch the LFC signal to the EVs by the dispatching method in the lower layer. The both dispatching methods of the LFC signal of the upper/lower layer are presented as follows:

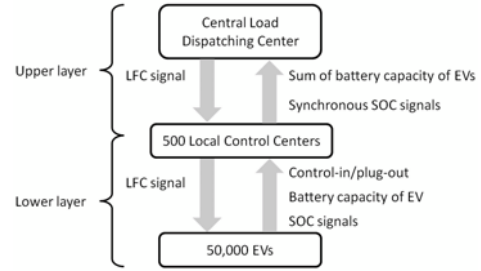


Figure 2: SOC synchronization control system.

In the dispatching method of the LFC signal in the lower layer, the charging and discharging priorities of the EVs are determined according to their SOC. The charging signal is dispatched to the EVs in ascending order of the SOC, whereas the discharging signal is dispatched in descending order of the SOC.

Figures 3 and 4 show examples of the dispatching method of the LFC signal in the lower layer when the LC center sends 60 kW of the charging LFC signal and 60 kW of the discharging LFC signal as shown in Figs. 3 and 4 respectively.

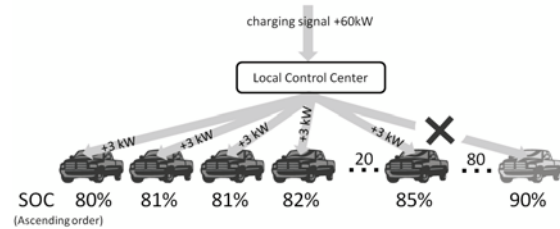


Figure 3: Example of dispatching method of 60kW charging signal in the lower layer.

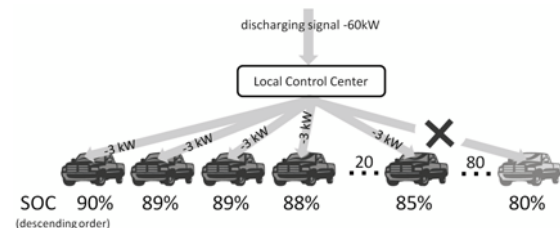


Figure 4: Example of dispatching method of 60kW discharging signal in the lower layer.

In the dispatching method of the LFC signal in the upper layer, the charging and discharging dispatching

priorities of the LC centers are determined according to their synchronous SOC (discussed in section 3.1). The charging signal is dispatched to the LC centers in ascending order of the synchronous SOC, whereas the discharging signal is dispatched in descending order of the synchronous SOC.

Figures 5 and 6 show examples of the LFC signal dispatching method in the upper layer when the CLDC sends 60 MW of the charging LFC signal and 60 MW of the discharging LFC signal respectively. The CLDC dispatches the LFC signal to the LC centers according to the number of the controllable EVs in each LC center.

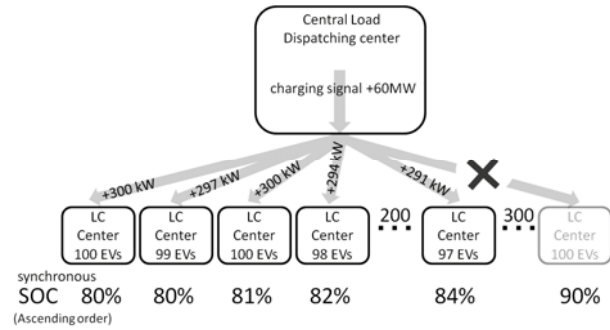


Figure 5: Example of dispatching method of 60MW charging signal in the upper layer.

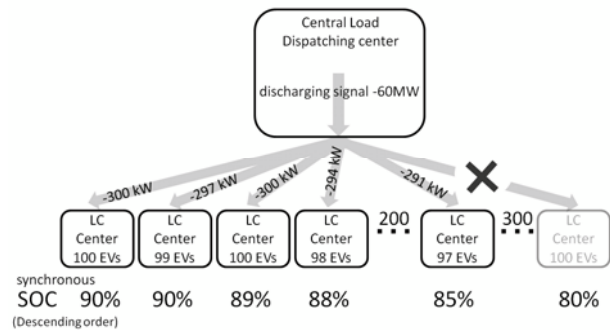


Figure 6: Example of dispatching method of 60MW discharging signal in the upper layer.

3 MODELING OF EVS IN V2G CONTROL SYSTEM

3.1 Evaluation of the SOC synchronization control in the lower layer

Two kinds of batteries of the EVs are assumed as shown in Table 1. Figure 7 shows the detailed EV model which stands for the behavior of the battery of one EV. The input to this model is the LFC signal dispatched to one EV in Fig. 2. The output is the power of one EV. In this subsection, one LC center and the EVs which are assigned into the LC center are simulated. C_{kw} is the inverter capacity (kW capacity: limit of charging and discharging power) of battery and C_{kWh} is the battery capacity (kWh capacity: limit of stored energy) of the battery in Fig. 7. The EV can be charged and discharged only within the range of $\pm C_{kw}$. However,

Energy of one EV hits the upper limit (90% of the SOC), the EV cannot be charged responding to the LFC signal. As well, Energy of one EV hits the lower limit (80% of the SOC). The EV cannot be discharged responding to the LFC signal.

The number of the controllable EVs ($N_{controllable}$) is fluctuated in association with the accumulated number of the control-in and plug-out of the EVs ($N_{control-in}$, $N_{plug-out}$) shown in (1). $N_{initial}$ is the initial number of controllable EVs. Their data are assumed to be plotted in Fig. 8 [3].

$$N_{controllable}(t) = N_{initial} - N_{plug-out}(t) + N_{control-in}(t) \quad (1)$$

Table 1: EV data.

	Type A	Type B
Inverter capacity of battery [kW]	3	3
Battery capacity of battery [kWh]	15	25
Installed rate [%]	34	66

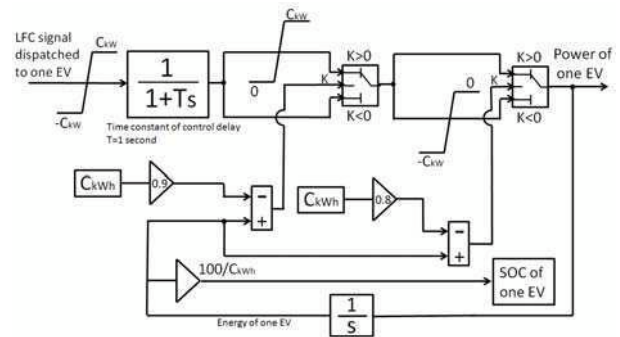


Figure 7: Detailed EV model.

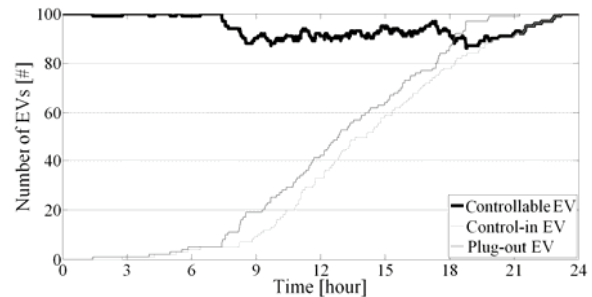


Figure 8: Accumulated number of control-in, plug-out, controllable EVs [3].

The SOC fluctuations of the 100 controllable EVs are simulated. The inverter capacity per EV is 3 kW and the total is 300 kW in this simulation. All the EVs are assumed to be controlled in at 85% of the SOC. The total LFC signal dispatched to the EVs is shown in Fig. 9. It is calculated by a random function. In this subsection, the 100 detailed EV models are used. Two cases are simulated. Case A is that the LC center makes the LFC signal dispatched to the EVs with the SOC synchronization control method in the lower layer as described in Figs. 3 and 4. Case B is that the LC center

generates the LFC signal dispatched to all the EVs equally without SOC synchronization control method.

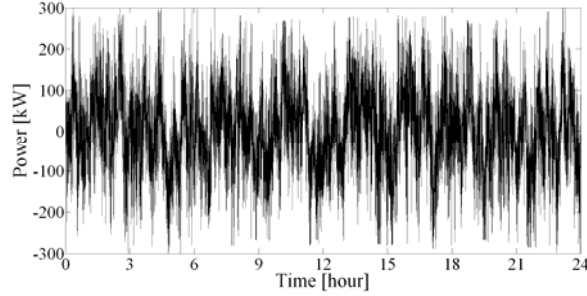


Figure 9: LFC signal.

Figure 10 shows the SOC of the EVs without the SOC synchronization control method. There are 100 lines in this figure. The mobility behaviors of the EVs are taken into account. The SOC of the EVs fluctuates parallel and disperse with time in Fig. 10. The SOC values of the EVs are plotted in Fig. 11, when the LC center dispatches the LFC signals in the lower layer by the SOC synchronization control method. As well, there are 100 lines in this figure. The lines become to coincide with the other in a short period in Fig. 11. It can be concluded from the results that the proposed control method synchronizes the SOC of the EVs.

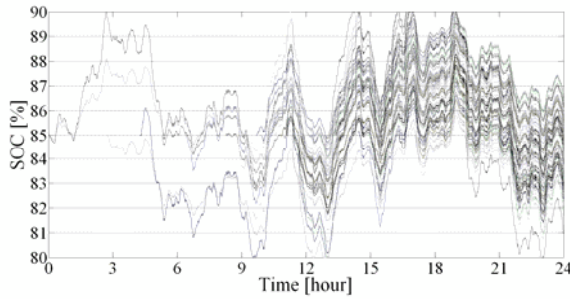


Figure 10: SOC of EVs without SOC synchronization control.

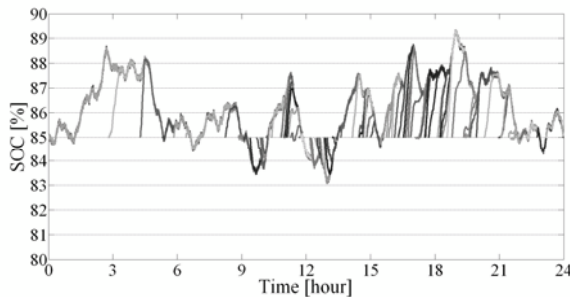


Figure 11: SOC of EVs with SOC synchronization control.

In this paper, we define the average of the SOC of the EVs in the SOC synchronization control in the lower layer as the *synchronous SOC of one LC center*.

3.2 Development of lumped model of EVs in one LC center

Figure 12 shows the lumped EV model in the lower layer which stands for the behavior of the batteries of the EVs in one LC center. The total charged/discharged

power of one LC center and synchronous SOC of the EVs in the controllable state are calculated by using this model. The stored energy model of one LC center enclosed by a double line in Fig. 12 is described in detail in Fig. 13, which calculates the total stored energy of the batteries of the EVs in one LC center.

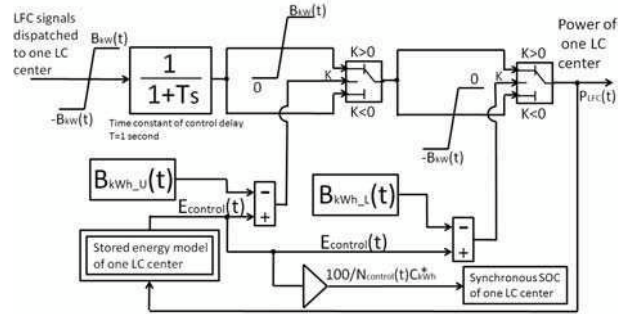


Figure 12: Lumped EV model.

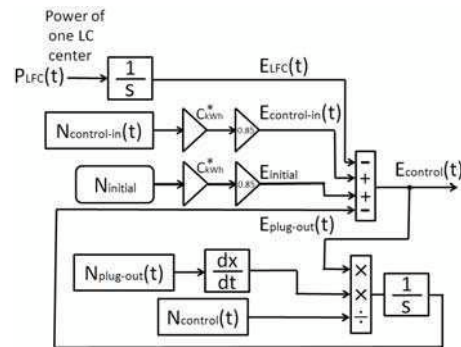


Figure 13: Stored energy model of one LC center.

The EVs cannot be charged/discharged over the inverter capacity of the batteries. The sum of the inverter capacity of the controllable EVs at each time is calculated from (2). If the energy of the EV is within the battery capacity, the EVs can respond to the LFC signal dispatched to the EVs within the range of $\pm B_{kW}$.

$$B_{kW}(t) = N_{control}(t) \cdot C_{kW}^* \quad [kW] \quad (2)$$

where $N_{control}$ is the number of the controllable EVs in Fig. 8. C_{kW}^* is the average inverter capacity of the controllable EVs.

The sum of battery capacity of the controllable EVs at each time is computed from (3). B_{kWh_L} is the lower limit calculated from (4) and B_{kWh_U} is the upper limit calculated from (5). C_{kWh}^* is the average battery capacity of the controllable EVs.

$$B_{kWh_L}(t) \leq E_{control}(t) \leq B_{kWh_U}(t) \quad (3)$$

$$B_{kWh_L}(t) = N_{control}(t) \cdot C_{kWh}^* \times 0.8 \quad [kWh] \quad (4)$$

$$B_{kWh_U}(t) = N_{control}(t) \cdot C_{kWh}^* \times 0.9 \quad [kWh] \quad (5)$$

Figure 13 shows the total energy model which generates the total stored energy of the controllable EVs as $E_{control}$ in Fig. 12. From Fig. 13, $E_{control}$ is calculated by the following equation.

$$E_{control}(t) = E_{initial} - E_{LFC}(t) + E_{control-in}(t) - E_{plug-out}(t) \quad (6)$$

where, $E_{initial}$ is the initial energy. E_{LFC} is the energy corresponding to the LFC signal and obtained by integrating the power of one LC center (P_{LFC}) by the following equation.

$$E_{LFC}(t) = \int_0^t P_{LFC}(\tau) d\tau \quad (7)$$

$E_{control-in}$ is the energy increase due to the EVs which change the state from the charging one to the controllable one (control-in). It is obtained by multiplying $N_{control-in}$ by the average charging energy ($0.85 \cdot C_{kWh}^*$). It is because all the EVs are changed to the charging state from the controllable state with the SOC of 85%. $N_{control-in}$ is the number of control-in EVs in Fig. 8.

$$E_{control-in}(t) = 0.85 \cdot C_{kWh}^* \cdot N_{control-in} \quad [kWh] \quad (8)$$

$E_{plug-out}$ is the energy decrease due to plug-out. The total energy of the EVs plugged out at time t is calculated from (9). E_i is stored energy of battery of each EV. $R_{plug-out}$ is differential value of $N_{plug-out}$ in Fig. 8.

$$\Delta E_{plug-out}(t) = \sum_{i=1}^{R_{plug-out}(t)} E_i(t) \quad (9)$$

When all the controllable EVs are synchronized, the energy of synchronized EVs and the average energy of all the controllable EVs (E^*) are the same. Therefore, $E_{plug-out}$ is calculated from (10).

$$\begin{aligned} E_{plug-out}(t) &= \int_0^t \Delta E_{plug-out}(\tau) d\tau \\ &= \int_0^t R_{plug-out}(\tau) \cdot E^*(\tau) d\tau \\ &= \int_0^t R_{plug-out}(\tau) \cdot \frac{E_{control}(\tau)}{N_{control}(\tau)} d\tau \quad [kWh] \end{aligned} \quad (10)$$

Figure 14 shows *the synchronous SOC of one LC center* shown in Fig. 11, which is calculated based on the SOC synchronization control, and that calculated from the lumped EV model in the lower layer shown in Fig. 12. Here, the LFC signal dispatched to the LC center shown in Fig. 9 is used. Both of the SOC's are almost the same. Therefore, the lumped EV model in the lower layer can approximate the actual total stored energy of the controllable EVs in the lower layer even if the EV users' uncertainty are considered.

3.3 Evaluation of the SOC synchronization control in the upper layer

In this subsection, supposing that the SOC's of the EVs are synchronized in the lower layer, the effectiveness of synchronization of a number of *the synchronous SOC of the LC center* is evaluated. The SOC fluctuation is simulated using 500 (the number of the LC center) lumped EV models whose parameters are tuned to those

of the LC center. For simplicity, the LFC signal calculated in the CLDC is 500 times of that shown in Fig 9. The CLDC makes the LFC signal dispatched to the LC center with the SOC synchronization control method in upper layer which is explained in Figs. 5 and 6.

Figure 15 shows the average of *the synchronous SOC of LC center* and the synchronous SOC whose deviation from the average is the largest of all. The result is similar to that shown in Fig. 14 because the same input signal is used. It can be said from Fig. 15 that the control enables a number of *the synchronous SOC of one LC center* to be synchronized in upper layer. These results conclude that the SOC's of all the controllable EVs are synchronized. In addition, SOC's of all the controllable EVs are approximated by using the lumped EV model shown in Fig. 12, whose parameters are tuned to those of all LC centers. The lumped model is used in next section.

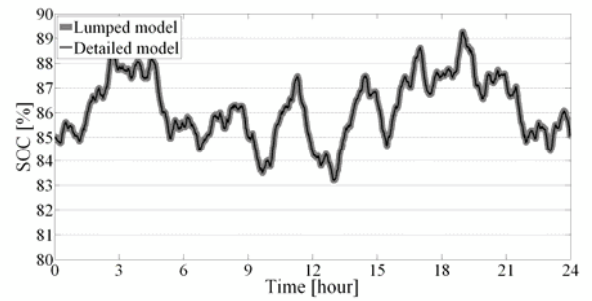


Figure 14: Average SOC of detailed models and SOC of the lumped model.

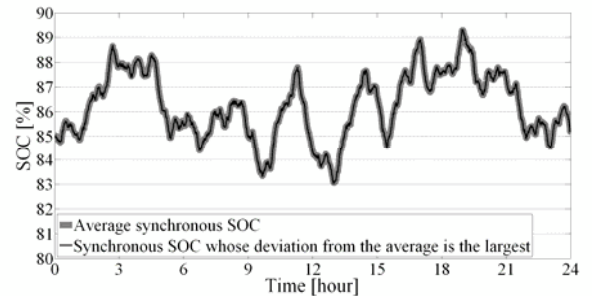


Figure 15: The synchronous SOC of the LCs with the SOC synchronization control.

4 EFFECTIVENESS OF FREQUENCY CONTROL IN V2G SYSTEM

4.1 Frequency analysis model

Figure 16 shows the frequency analysis model used in this paper. It can be used for the simulation in the period from several hours to a day. This model consists of the equivalent generator model, the thermal power plant model [4], the wind power generation output, the photovoltaic generation output, the load fluctuation, the EDC system model [4], the LFC system model and the EV model. The equivalent generator model has an inertia constant M_{eq} equal to the sum of the inertia constants of all the generators. It is updated according to the total

capacity of the connected generators. The load-damping coefficient D is updated according to the total load demand. The input into the EV model is the total control signal whereas the output is the total power from EVs.

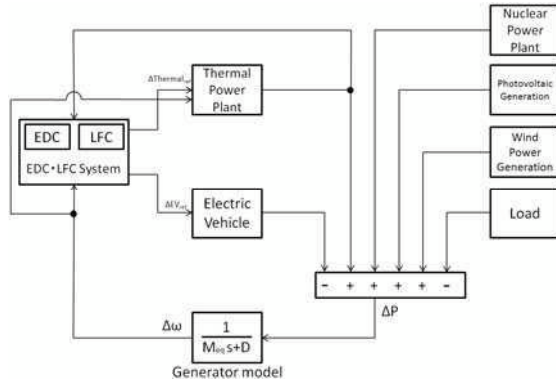


Figure 16: Frequency analysis model.

As shown in Fig. 17, the LFC system model generates the LFC signal basically from the Area Requirement (AR). This AR is computed from the imbalance between supply and demand. The LFC signal is then sent to the thermal power plants. Moreover, as seen from Fig. 17, there is a portion where the thermal power plants cannot compensate. Therefore, the LFC signal is also dispatched to the EVs to make up for this portion.

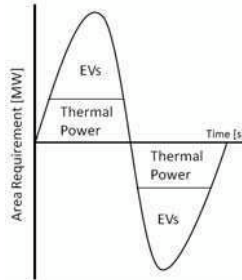


Figure 17: The CLDC and the LC center.

4.2 Simulation condition and results

The simulation condition of the frequency analysis is as follows. The system data is summarized in Table 2. Table 3 shows the generator model data. The nuclear power plant output is constant as 3,800MW. The total rated capacity of the thermal generators connected into the power system changes in proportion to the power output as shown in Fig. 18. It is updated every 30 minutes to 1.25 times as much as the power output to the thermal generators at that time. Fig. 19 plots the net system load fluctuation including the wind power output and PV output considered as negative loads. The simulation period is 24hours on sunny weekday. In the study area, there are 50,000 EVs and 500 LC centers. The total capacity of EVs is 150MW/1080MWh. The total controllable capacity of EVs is 150MW/108MWh which changes according to the number of controllable EVs.

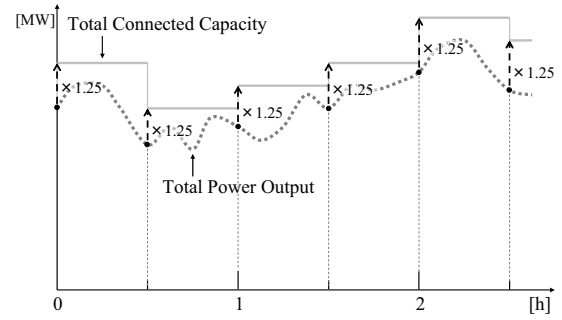


Figure 18: Setting of total connected capacity of thermal plants into the grid.

Table 2: System data.

	Rated Capacity [MW]
Nuclear plant	4,000
Thermal plant (MAX)	12,000
Wind power generation	2,000
Photovoltaic generation	2,000
BESS (Case 2)	150(1080MWh)

Table 3: Generator model data.

Inertia constant of thermal plants (machine base)	9.01 s
Inertia constant of nuclear plants (machine base)	9.03 s
Load-damping coefficient D	2.0 p.u.

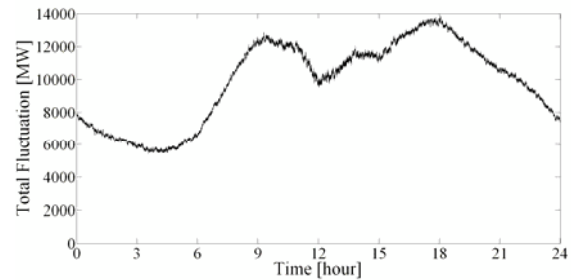


Figure 19: Net load fluctuation.

The numerical simulations are carried out in three cases. In Case 1, EVs are not controlled. In Case 2, the EVs are controlled with the SOC synchronization control. In Case 3, the EVs are not controlled but the BESS whose capacity is 150MW/1080MWh is penetrated.

Here, the performance on suppression of the system frequency fluctuation is measured by the maximum value of frequency deviation and the Root Mean Square (RMS) value as written in (11).

$$x_{rms} = \sqrt{\frac{1}{N} \sum_{i=1}^N \Delta f_i^2} \quad (11)$$

where N is the number of samples, and Δf_i is the frequency deviation of the sample i .

The total power of the EVs calculated from the EV model in Case 2 is shown in Fig. 20. It can be seen that the total power is controlled according to the LFC sig-

nal. The frequency fluctuations and their indices in three cases are shown in Figs. 21 to 23 and Table 3. It can be seen from Figs. 21, 22 and Table 3 that when the EVs are controlled with the SOC synchronization control, the frequency fluctuation is suppressed.

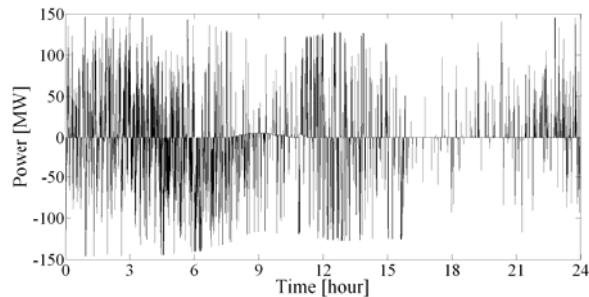


Figure 20: Total output power of the EVs.

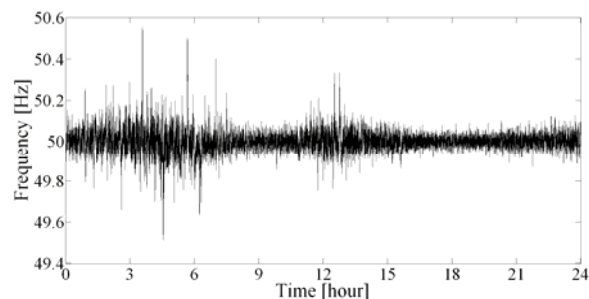


Figure 21: Frequency fluctuation in Case 1.

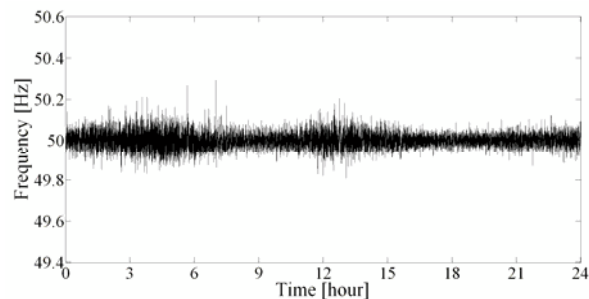


Figure 22: Frequency fluctuation in Case 2.

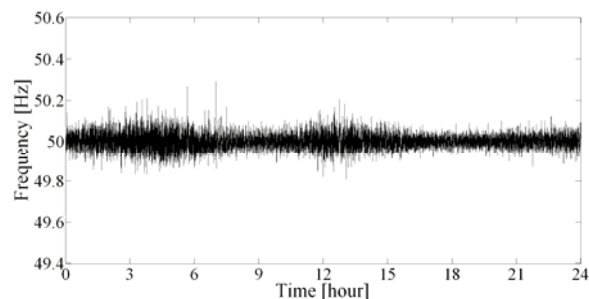


Figure 23: Frequency fluctuation in Case 3.

In comparison between Case 2 and Case 3, the effectiveness of the SOC synchronization control is nearly equal to that of the equivalent BESS. The difference of the RMS value between Case 2 and Case 3 shown in Table 3 is caused by the change of the total controllable capacity of EVs

Table 4: MAX and RMS value of frequency fluctuation.

	MAX [Hz]	RMS [Hz]
Case 1	0.553	0.0509
Case 2	0.293	0.0332
Case 3	0.293	0.0330

5 CONCLUSION

This paper has proposed a new SOC synchronization control method of EVs. In addition, the effectiveness of the V2G control on the frequency regulation in the power system has been made cleared. In this paper, the EV users' convenience and uncertainties are considered. The power system does not need to consider some of the EVs which are plugged-out or stop charging/discharging due to their full/empty battery energy and the CLDC does not need to know the SOC of each EV. The future work is to control the EVs in cooperation with the other controllable loads such as heat pump water heaters.

In the power system with a large penetration of renewable sources, the local control such as distribution voltage control could conflict with the global one such as frequency control. It is important to consider the coordination of the local control and the global control in power systems in the future work

REFERENCES

- [1] W. Kempton, V. Udo, K. Huber, K. Komara, S. Letendre, S. Baker, D. Brunner, and N. Pearre: "A Test of Vehicle-to-Grid(V2G) for Energy Storage and Frequency Regulation in the PJM System", Publication of MAGICC(Mid-Atlantic Grid Interface Cars Consortium), http://www.magicconsortium.org/_Media/test-v2g-in-pjm-jan09.ppd (2009)
- [2] Y. Ota, H. Taniguchi, T. Nakajima, K. M. Liyanage, K. Shimizu, T. Masuta, J. Baba: "Autonomous Distributed Vehicle-to-Grid for Ubiquitous Power Grid and its Effect as a Spinning Reserve", 16th International Conference on Electrical Engineering, PEVs-01, Busan, Korea, July. 2010
- [3] Road Bureau, Ministry of Land, Infrastructure and Transport, "ROAD TRAFFIC CENSUS 2005", <http://www.mlit.go.jp/road/ir/ir-data/ir-data.html>
- [4] T. Masuta, A. Yokoyama, and Y. Tada, "System Frequency Control by Heat Pump Water Heaters (HPWHs) on Customer Side Based on Statistical HPWH Model in Power system with a Large Penetration of Renewable Energy Sources", in Proc. 2010 International Conference on Power System Technology, 0674, Hangzhou, China, Oct. 2010